

**RIFT VALLEY IN THE ATLANTIC OCEAN NEAR 36° 50'N:  
PETROLOGY AND GEOCHEMISTRY OF BASALTIC ROCKS\***H. BOUGAULT and R. HEKINIAN  
*Centre Océanologique de Bretagne, Brest (France)*

Received September 4, 1974

Dredged rocks from an area of about 15 km<sup>2</sup> within the inner floor and on the adjacent walls of the Rift Valley were collected. Based on petrographic and chemical data, four types of basaltic rocks were recognized: (1) picritic basalts with olivine xenocrysts, TiO<sub>2</sub> < 0.6%, K<sub>2</sub>O < 0.1%, (2) olivine basalts with olivine megacrysts, TiO<sub>2</sub> = 0.8–1.5%, K<sub>2</sub>O = 0.1–0.2%, (3) highly phyrlic and moderately phyrlic plagioclase basalts with megacrystic plagioclase, TiO<sub>2</sub> < 1.3%, K<sub>2</sub>O < 0.3%, and (4) pyroxene basalts with pyroxene > plagioclase, TiO<sub>2</sub> = 0.8–1%, K<sub>2</sub>O = 0.2–0.4%. The Cr and Ni having high partition coefficients show different variation trends for each type of rock and their values decrease continuously as crystallization proceeds within each type of basalt. It is speculated that two different magmas have given rise to the above-mentioned rocks. One has yielded the picritic basalts and subsequently the olivine basalts after a separation of the olivine cumulates; the other gave rise to the plagioclase basalts.

**1. Introduction**

Since the discovery of the Rift Valley in the Atlantic Ocean [1] little information has been gathered from the inner floor of the Rift Valley, locus of emplacement of new oceanic crust [2]. Even if the North Atlantic Ocean represents one of the most dredged parts of the world's ocean, only five rock stations, to our knowledge, are located in the inner floor of the Rift Valley and from which suitable data has been published [3–5]. This fact is probably due to the narrowness of the inner floor and the difficulty of positioning dredge hauls.

An area of approximately 28 km along the Rift Valley at about 36°N in the Atlantic Ocean was explored in 1972 by the R.V. "Jean Charcot" in order to gather information as a contribution to the French–American Mid-Ocean Undersea Survey (Famous) program. The rift valley in the area of study is located between two fracture zones, which are more than 7 km away from the survey zone, and the inner floor

is limited by two walls which are about 1500 m above the intersection with the inner floor. Linear features with a regional gradient of less than 6° lie on the wall of the Rift Valley and have the appearance of blocks or steps on which ridges or individual hills are superimposed [6, 2].

Four dredge hauls (DR2, DR3, DR6, DR7) were collected from the eastern and western walls of the Rift Valley at a depth varying between 1800 and 2200 m (Table 1). Dredges 5, 9, 10 and 11 were taken from the intersection of the walls and the inner floor of the Rift Valley at a depth of about 2400–2800 m (Table 1). The inner floor in the area of survey is made up of deeps and a line of hills called the "Central High" [6]. Three dredges (DR1, DR4, DR8) were collected near or on the flanks of the central high at about 2500 m and one dredge, DR12, was taken in a deep on the eastern side of the inner floor (Table 1).

It is the purpose of this paper to point out some of the differences that exist as far as the compositional variation of rocks is concerned within this limited area about 15 km<sup>2</sup> of the Rift Valley near 36°N. Mineralogical and chemical methods have been used to show the presence of different types of basalts and their possible relationship.

\* Contribution no. 308 of the Département Scientifique, Centre Océanologique de Bretagne.

TABLE 1

Locations and depths of dredges (CH 31) from the Rift Valley in the Atlantic Ocean near 36°N.

Dredge No.	Province	Latitude N	Longitude W	Depth (m)	Type of rocks
DR1	inner floor	36° 50'	33° 16'	2700–2800	olivine basalts
DR2	eastern wall	36° 47' 6	33° 15' 5	2150–2350	plagioclase, pyroxene and olivine basalts
DR3	eastern wall	36° 47' 35	33° 13' 05	1850–2100	pyroxene and plagioclase basalts
DR4	inner floor	36° 49' 72	33° 15' 92	2650–2730	olivine basalts
DR5	foot of eastern wall	36° 46'	33° 16' 5	2500–2630	olivine basalts
DR6	western wall	36° 46' 83	33° 18' 43	1900–2300	plagioclase and pyroxene basalts
DR7	western wall	36° 47' 10	33° 21' 25	1800–1900	plagioclase basalts.
DR8	inner floor	36° 50' 30	33° 14' 65	2780–2820	picritic basalts and olivine basalts
DR9	foot of the western wall	36° 52' 40	33° 15' 15	2600–2840	olivine basalts
DR10	foot of the western wall	36° 52' 25	33° 14' 55	2380–2700	pyroxene and plagioclase basalts
DR11	foot of the eastern wall	36° 49' 3	33° 15' 0	2600–2720	olivine basalts
DR12	inner floor	38° 52	33° 14' 9	2840–2950	picritic basalts and olivine basalts

## 2. Petrological description

Most of the specimens collected by dredging from 36°N are fragments of pillow lava which show columnar jointing and chilled margins in various degrees of preservation. Curved slabs of about 3–6 cm thick which represent fragments of lava tubes were collected from station DR11 [7]. The fact that the slabs with

glassy margins are fragments of walls of lava tubes was confirmed by the 1973 Archimède dives [2]. Another type of rock with different surface morphology consists of small fragments (< 20 cm in diameter) showing a rough surface (similar to "aa" type) which is abundantly vesiculated and coated with palagonite and manganese.

Although the majority of the rocks are low-potassi-

TABLE 2

Modal analyses of rocks from Leg CH 31 of R.V. "Jean Charcot" in the Rift Valley near 36°N

Rock types	Plagioclase basalts			Olivine basalts		Pyroxene basalts			
	Sample No:	DR2-132	DR3-131	DR10-100C	DR5-304	DR9-308	DR3-123	DR10-310	DR10-105
Plagioclase									
phenocryst		28.1	29.6	11.5		4.9			
microphenocryst		2.3	1.4	2.4		0.8			0.6
matrix		6.3	16.6	29.3	25.4	19.1	33.6	28.6	31.8
Pyroxene									
phenocryst		7.1	2.3	2.7					
matrix		0.6	45.3	34.2		5.8	50.5	57.6	60.8
Olivine									
phenocryst					2.4	3.0			
matrix		1.4		0.3	19.3	7.5			
Fe ore		10.7	6.8	9.8	7.4	13.1	12.6	12.4	9.8
Palagonite		0.2	1.9	1.6			0.4		
Mesostasis*		43.28	1.4	8.0	45.5	46.6	2.7	1.4	

\* Mesostasis includes iron oxide minerals, glass and cryptocrystalline aggregates. The plagioclase phenocrysts of the plagioclase basalts include megacrystic plagioclase.

um tholeiites (0.1–0.4%) there is strong evidence in terms of the mineral constituents, the major oxide variations, and the trace element study that we may further subdivide these rocks into four different types of basalts.

*Picritic basalts*: normative and modal olivine > 20% with megacrysts, phenocrysts, microphenocrysts, matrix olivine.  $\text{Al}_2\text{O}_3 < 14\%$ .

*Olivine basalts*: 2% < normative and modal olivine < 16%, with phenocrysts, microphenocrysts, matrix olivine.  $14\% < \text{Al}_2\text{O}_3 < 16\%$ .

*Plagioclase basalts*: normative and modal plagioclase > normative and modal pyroxene, with megacrysts of plagioclase,  $\text{Al}_2\text{O}_3 > 15\%$  (Tables 2, 4).

*Pyroxene basalts*: normative and modal pyroxene > normative and modal plagioclase,  $\text{Al}_2\text{O}_3 < 16\%$  (Tables 2, 4).

Shido et al [8] have suggested a similar type of classification in distinguishing low-potash olivine tholeiites from tholeiites enriched in plagioclase. Hekinian and Aumento [9] using petrographic and major element variations have emphasized the presence of pyroxene basalts within the M.A.R. rocks near 53°N.

### 2.1. Picritic basalts

The picritic basalts were dredged from the inner floor of the Rift Valley. The name picritic basalts is given here to rocks that consist of abundant large olivine crystals (> 25%) set in a groundmass of a dark mesostasis, tiny plagioclase laths, olivine, and glass. The large olivine crystals reaching up to 1 cm in diameter occur either as cumulates or as individual crystals. Most of these are resorbed with rounded edges. In addition to the megacrysts there are smaller olivine crystals (< 2mm in diameter) showing well-developed crystalline outlines. The composition of the olivine megacrysts in percent forsterite molecule content is about  $\text{FO}_{90}$ . Olivine also occurs as euhedral phenocrysts and microphenocrysts. The plagioclase is primarily concentrated in the matrix where it forms tiny laths comprising less than 2% of the bulk rock. Large rounded resorbed plagioclase are occasionally seen. Euhedral and resorbed crystals of reddish brown spinel occur at the margin of olivine, rarely as inclusions in olivine or as isolated crystals in the matrix. Inclusions of glass are often present in olivine crystals. These picritic basalts are characterized by a low  $\text{TiO}_2$  (< 0.6%),

a low  $\text{K}_2\text{O}$  (< 0.1%), and low  $\text{Al}_2\text{O}_3$  content (< 14%) (Table 3).

### 2.2. Olivine basalts

The olivine basalts are most abundant on the inner floor of the Rift Valley. The olivine basalts are mineralogically not well defined because in the sample studied here the rocks belonging to this category are not well crystallized (Table 2). Hence the criteria used here for their classification of olivine basalts is mainly based on the normative mineral content. The composition of the olivine given in percent forsterite molecule is about  $\text{FO}_{90}$ . The texture of these rocks is either variolitic or intersertal. Olivine usually occurs as phenocrysts ( $2V = 82^\circ - 87^\circ$ ) and micro-phenocrysts associated with plagioclase. The matrix of these rocks consists of glass, dark mesostasis, small olivine, tiny plagioclase laths and a few clinopyroxene granules (Table 2). The chemistry of the olivine basalts is characterized by an  $\text{Al}_2\text{O}_3$  content less than 16% by a  $\text{K}_2\text{O}$  content less than 0.20%, and a  $\text{TiO}_2$  content between 0.8 and 1.5% (Table 3).

### 2.3. Plagioclase basalts

The plagioclase basalts are phaneritic and sometimes have slightly rounded edges. Many of these rocks are coated with a film of manganese oxide. They also contain traces of hematite and palagonite which indicates that these rocks have undergone some degree of weathering.

Two types of plagioclase basalts have been recognized: (1) the highly phyric basalts containing megacrysts of plagioclase comprising up to 30% of the bulk rock, and (2) the moderately phyric basalts containing few megacrysts of plagioclase (< 20%).

(1) The highly phyric plagioclase basalts collected from the walls of the Rift Valley are characterized by large plagioclase crystals reaching up to 1.2 cm in diameter. The larger plagioclase are resorbed and often show rounded edges. These megacrysts often show a thin rim of a more sodic plagioclase. Plagioclase basalts are usually depleted in olivine, and augite is colorless with  $2V = 41^\circ - 61^\circ$ . When the matrix is well crystallized, it has equal amounts of clinopyroxene and plagioclase laths. The textural feature of the matrix is either hyalopilitic, intergranular or subophitic. Four generations of plagioclase are encountered in these rocks: megacrysts,

TABLE 3  
Chemical analyses (wt. %) of basaltic rocks from the Rift Valley in the Atlantic Ocean near 36°N

	Picritic basalts		Olivine basalts														
	DR12 -320	DR12 -316	DR11 -315	DR11 -315A	DR4 -303	DR5 -100B	DR5 -304	DR8 -314	DR1 -122	DR9 -308	DR9 -319	DR9 -322 inter.	DR9 -322 margin	DR2 -174	DR9 -309	DR1 -124	
SiO <sub>2</sub>	46.27	47.45	49.70	50.24	49.34	49.93	50.33	49.79	50.45	49.96	49.83	49.92	49.94	50.62	49.28	49.55	
Al <sub>2</sub> O <sub>3</sub>	14.20	13.49	14.86	14.72	14.75	14.53	14.92	14.86	15.40	14.83	14.82	15.29	15.04	14.84	15.30	15.19	
Fe <sub>2</sub> O <sub>3</sub>	1.20	1.04	1.65	0.98	0.91	1.45	1.43	1.39	1.37	1.46	1.35	1.66	1.34	1.56	1.68	1.41	
FeO	7.69	7.72	9.28	9.50	7.42	8.62	7.71	8.32	7.41	8.06	9.37	8.03	8.24	8.76	1.44	7.48	
MnO	0.17	0.17	0.18	0.18	0.18	0.18	0.18	0.18	0.18	0.18	0.18	0.18	0.18	0.18	0.18	0.18	
MgO	16.06	16.65	8.23	8.24	11.00	9.22	10.12	9.54	9.33	9.82	8.44	9.12	9.02	8.12	9.20	10.53	
CaO	11.89	11.42	11.90	11.82	11.48	12.08	11.89	12.51	12.26	12.43	11.82	12.55	12.59	11.95	12.70	12.18	
Na <sub>2</sub> O	1.98	0.37	2.28	2.14	1.55	2.34	1.79	2.18	2.23	2.01	2.28	2.23	2.08	1.91	2.55	2.51	
K <sub>2</sub> O	0.09	0.08	0.22	0.23	0.16	0.23	0.17	0.22	0.16	0.12	0.23	0.13	0.13	0.24	0.17	0.15	
TiO <sub>2</sub>	0.62	0.59	1.45	1.44	0.86	1.27	1.07	1.09	0.90	1.02	1.44	1.04	1.04	1.41	1.02	0.91	
P <sub>2</sub> O <sub>5</sub>	0.07	0.09	0.18	0.18	0.10	0.18	0.10	0.12	0.11	0.12	0.18	0.10	0.10	0.18	0.13	0.12	
PF	0.48	0.53	0.62	0.55	0.84	0.72	0.69	0.52	0.51	0.65	0.57	0.63	0.62	0.70	0.79	0.51	
Total	100.74	100.59	100.54	100.21	98.58	100.74	100.39	100.71	100.30	100.65	100.50	100.87	100.31	100.46	100.43	100.71	
<i>Norm</i>																	
Qtz	0.00	0.00	0.00	0.00	0.00	0.00	0.00	0.00	0.00	0.00	0.00	0.00	0.00	1.36	0.00	0.00	
Ne	2.41	0.00	0.00	0.00	0.00	0.00	0.00	0.00	0.00	0.00	0.00	0.00	0.00	0.00	0.00	0.00	
Or	0.53	0.47	1.30	1.35	0.94	1.35	1.00	1.30	0.94	0.70	1.35	0.76	0.76	1.41	1.00	0.88	
Ab	12.29	11.59	19.29	18.10	13.11	19.80	15.14	18.44	18.86	17.00	19.29	18.86	17.60	16.16	21.57	21.23	
An	29.59	30.42	29.66	29.88	32.81	28.46	32.17	30.11	31.53	31.08	29.52	31.32	31.31	31.21	29.79	29.73	
Di	wo	12.08	10.70	11.77	11.51	9.80	12.64	10.92	13.01	11.92	12.43	11.66	12.64	12.72	11.23	13.50	12.48
	en	8.44	7.50	6.75	6.45	6.38	7.66	6.99	8.00	7.51	7.78	6.68	7.79	7.70	6.55	8.56	8.10
Hyl	fs	2.62	2.29	4.48	4.59	2.74	4.29	3.20	4.26	3.66	3.89	4.46	4.11	4.33	4.14	4.08	3.52
	en	0.00	6.60	10.90	12.15	17.74	8.27	16.66	7.53	10.86	11.18	9.73	8.54	10.15	13.67	2.69	4.77
Fo	0.00	2.01	7.24	8.64	7.63	4.63	7.63	4.01	5.29	5.60	6.50	4.51	5.71	8.65	1.28	2.07	
Fa	22.11	19.16	1.98	1.33	2.29	4.92	1.07	5.75	3.39	3.84	3.22	4.46	3.23	0.00	8.16	9.35	
Mt	7.56	6.44	1.45	1.04	1.08	3.04	0.54	3.38	1.82	2.12	2.37	2.59	2.00	0.00	4.28	4.48	
Mt	1.73	1.50	2.39	1.42	1.31	2.10	2.07	2.01	1.98	2.11	1.95	2.40	1.94	2.26	2.43	2.04	
Ilm	1.17	1.12	2.75	2.73	1.63	2.41	2.03	2.07	1.70	1.93	2.73	1.97	1.97	2.67	1.93	1.72	
Ap	0.16	0.21	0.42	0.42	0.23	0.42	0.23	0.28	0.25	0.28	0.42	0.23	0.23	0.42	0.30	0.28	

phenocrysts, microphenocrysts and matrix plagioclase. The phenocrysts and the microphenocrysts show well-defined crystalline outlines. The anorthite content of the plagioclase megacrysts varies between  $An_{83}$  and  $An_{88}$  while that of the plagioclase phenocrysts is about  $An_{46}$ – $An_{66}$ . The plagioclase laths in the matrix are associated with a dark mesostasis of clinopyroxene granules in the more crystalline specimens. The matrix of these specimens show textural features similar to that of pyroxene basalts. The plagioclase containing a large amount of plagioclase megacrysts are characterized by a high  $Al_2O_3$  content (up to 21%), a low  $TiO_2$  ( $< 0.8\%$ ) and  $K_2O$  ( $< 0.15\%$ ) values (Table 3).

(2) The moderately phryic basalts also falling in the same category on the basis of their normative plagioclase content consist of relatively small ( $< 2$  mm length) plagioclase phenocrysts ( $< 20\%$ ) and have a matrix enriched in plagioclase (DR10-314, DR10-100, DR10-311). They differ from the xenocrystic plagioclase basalts by their lower  $Al_2O_3$  content ( $< 17\%$ ) higher  $K_2O$  content ( $> 0.20\%$ ) and a  $TiO_2$  content of about 1% (Table 3).

#### 2.4. Pyroxene basalts

Usually the pyroxene basalts have a rough weathered surface with sharp edges and coated with manganese oxide. Common fragments of pillow lava with columnar jointings also occur. The "aa" like basalts are finer grained (0.4 mm in average diameter) than those having columnar jointing. The pyroxene basalts are aphanitic hypocrySTALLINE and holocrystalline with an intersertal and subophitic texture. Usually the amount of clinopyroxene is equal to or higher than the amount of plagioclase (Table 2). No large plagioclase crystals such as those found in the plagioclase basalts were observed in these rocks. However, sometimes an agglomeration of plagioclase microphenocrysts and pyroxene occurs (sample DR2-301). In the most crystalline rock the modal content of clinopyroxene reaches up to 50% while the plagioclase content is less than 35% (Table 2). The clinopyroxene is colorless and consists of an augitic diopside. The iron oxide mineral content is slightly higher (about 12%) than that of the plagioclase basalts (Table 2). The pyroxene basalts have a relatively low  $Al_2O_3$  content ( $< 16\%$ ) a  $TiO_2$  content between 0.8 and 1% and a  $K_2O$  higher than 0.20% (Table 3).

### 3. Major and minor element variations

The samples studied here are relatively fresh as suggested by their ignition loss. The weight of oxygen necessary to oxidize FeO is generally higher than that of the water content giving rise to a negative ignition loss. The major and minor element variations are shown in Table 3. Two diagrams are used to show the different types of rocks encountered in the dredge hauls. A ternary plagioclase–pyroxene–olivine diagram is shown in Fig. 1. This diagram is similar to the system diopside–forsterite–anorthite of Osborn and Tait [11]. Similarly, Shido et al. [8] and Miyashiro et al. [10] have shown the distribution of plagioclase tholeiites and olivine tholeiites separated by a "cotectic" line in a plagioclase–pyroxene–olivine diagram. The plots of the different types of basalts encountered are separated by arbitrary boundaries corresponding to the "cotectic lines" mentioned by Shido et al. [8]. This ternary diagram (Fig. 1) reproduces only the plots of the chemical composition of the bulk rock calculated as the norms. This diagram helps to distinguish and visualize the four different rock types encountered. The plagioclase and picritic basalts, both containing abundant megacrystic material are plotted on two distinct fields (Fig. 1). Olivine basalts are separated from both pyroxene basalts and plagioclase basalts (Fig. 1). The composi-

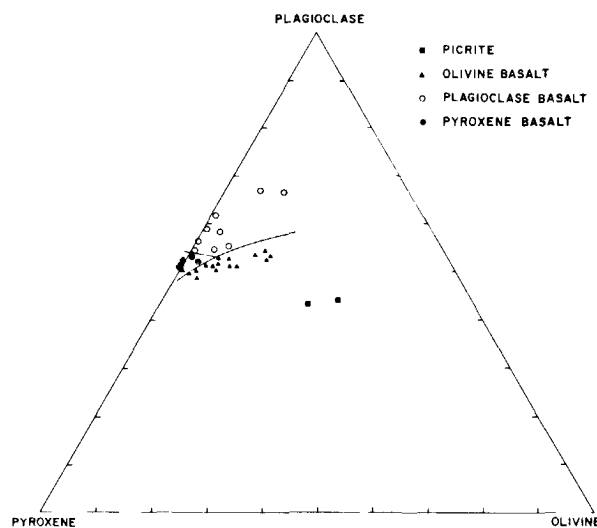


Fig. 1. Pyroxene–plagioclase–olivine triangular diagram showing the field of plagioclase basalts, olivine basalts, pyroxene basalts and picritic basalts.

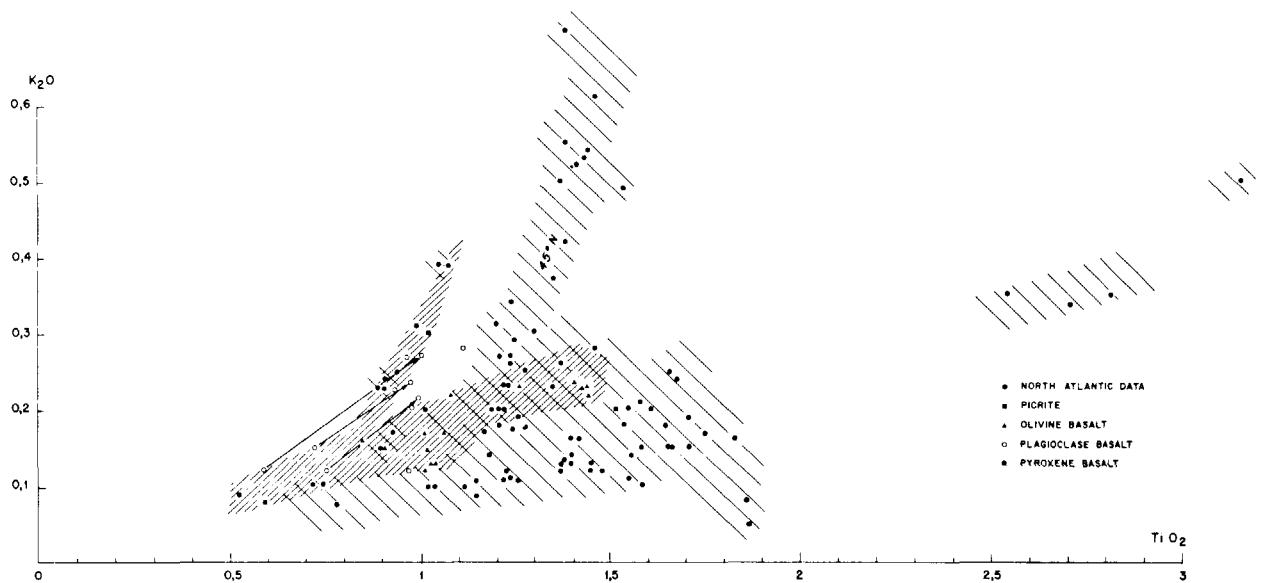


Fig. 2.  $K_2O$ – $TiO_2$  variation diagram showing the plots of the basaltic rocks from the North Atlantic Ocean (●) [3–5, 7, 8, 10, 12–15]. Samples from  $36^\circ N$  have the same symbols as in Fig. 1. The tie line between two empty circles indicates the recalculated plagioclase basalts megacrysts-free values.

tion of the groundmass of plagioclase basalts would fall near or in the field of pyroxene basalts. This is also evidenced by the fact that the matrix of plagioclase basalts show similar features to that of the pyroxene basalts.

The  $K_2O$ – $TiO_2$  diagram (Fig. 2) also has been found useful to distinguish and to speculate on the relationship between these different types of rocks already shown in the above pyroxene–plagioclase–olivine ternary diagram. Fig. 2 shows the plot of rocks dredged from  $36^\circ N$  and other published analyses from the North Atlantic [3–5, 7, 8, 10, 12–15]. Most of the published data, and those from  $36^\circ N$  including the picritic and olivine basalts plot on a large  $TiO_2$  (0.5–2%) and a narrow  $K_2O$  (0.5–2.5%) content variation trend. Basalts from  $45^\circ N$  plot on a separate trend with a narrow  $TiO_2$  (1.15–1.4%) and high  $K_2O$  (0.25–0.7%) variation trends. Similarly pyroxene basalts from  $36^\circ N$  plot in a parallel trend to the  $45^\circ N$  basalts ( $TiO_2 = 0.8$ – $1\%$ ,  $K_2O = 0.2$ – $0.4\%$ ) (Fig. 2). The bulk composition of plagioclase basalts from  $36^\circ N$  plot on the trend of the olivine basalts. The values of the groundmass after separating the large megacrysts plot in the field of the pyroxene basalts (Fig. 2). It is interesting to notice that the plagioclase basalt without plagioclase megacrysts would also plot in or near the field of the pyroxene basalts.

#### 4. First-series transition elements

The first-series transition metals have been found helpful to distinguish the different types of basalts mentioned above. In addition the study of these transition elements may give further information for determining the relationship within and between the various rock types.

##### 4.1. Partition coefficients

The analyses of major and first transition series elements were made on separated minerals and glass or mesostasis of different types of basalts (Tables 4, 5). It was assumed that crystals and glass or mesostasis were in equilibrium and this was confirmed by the order of magnitude of the partition coefficients found, especially for Cr and Ni in the olivine or the pyroxene crystals. The olivine megacrysts of the picritic basalts appear to be in equilibrium with the glassy portion of the rock.

The calculation of partition coefficients assumes that the mineral phases are homogeneous, and hence the possible effects of diffusion during crystallization as pointed out by Albarède and Bottinga [16] is not taken into account. In this way, the partition coefficients are considered as a mass balance between phases

TABLE 4

Chemical analyses (wt. %) of basaltic rocks from the Rift Valley in the North Atlantic Ocean near 36°N (DR10-311, DR10-314 and DR10-100C contain less than 20% plagioclase phenocrysts)

	Pyroxene basalts						Plagioclase basalts						
	DR2-301	DR3-123	DR6-305	DR6-306	DR10-105	DR10-310	DR3-321	DR7-318	DR10-311	DR10-314	DR2-132	DR3-131	DR10-100C
SiO <sub>2</sub>	50.32	50.46	50.32	49.27	50.58	50.19	48.52	46.76	49.51	49.10	49.65	49.24	49.31
Al <sub>2</sub> O <sub>3</sub>	15.03	14.81	14.69	14.57	14.54	14.27	20.99	19.46	15.77	15.89	19.25	18.30	17.04
Fe <sub>2</sub> O <sub>3</sub>	2.35	1.92	2.58	1.76	1.78	2.22	1.21	2.99	2.32	2.73	1.24	2.00	2.04
FeO	6.45	6.71	6.86	7.90	7.85	7.61	4.67	5.58	6.54	6.60	5.51	5.24	6.15
MnO	0.18	0.18	0.18	0.18	0.18	0.18	0.12	0.18	0.18	0.18	0.10	0.12	0.15
MgO	8.26	8.07	8.00	8.44	8.35	8.18	6.59	6.75	8.78	8.67	6.90	7.96	8.17
CaO	13.68	13.26	12.89	12.50	12.67	12.43	15.03	14.10	12.81	13.10	14.60	14.32	13.42
Na <sub>2</sub> O	1.84	2.34	2.42	2.65	1.91	1.74	1.88	2.23	2.28	1.98	1.80	1.60	1.61
K <sub>2</sub> O	0.32	0.23	0.40	0.25	0.30	0.31	0.12	0.12	0.23	0.28	0.12	0.15	0.27
TiO <sub>2</sub>	1.02	0.90	1.09	0.98	1.03	1.00	0.59	0.98	0.99	1.15	0.75	0.73	0.97
P <sub>2</sub> O <sub>5</sub>	0.16	0.11	0.13	0.12	0.11	0.12	0.07	0.19	0.14	0.13	0.11	0.08	0.15
PF	1.15	1.01	1.28	0.73	0.90	1.05	0.67	1.32	0.90	1.12	0.61	1.09	1.05
Total	100.75	99.99	100.83	99.34	100.19	99.29	100.56	100.65	100.44	100.99	100.63	100.82	100.32
<i>Norm</i>													
Qtz	0.88	0.00	0.00	0.00	0.65	2.08	0.00	0.00	0.00	0.00	0.00	0.00	0.48
Ne	0.00	0.00	0.00	0.00	0.00	0.00	0.00	0.06	0.00	0.00	0.00	0.00	0.00
Or	1.89	1.35	2.36	1.47	1.77	1.83	0.70	0.70	1.35	1.65	0.70	0.88	1.59
Ab	15.56	19.80	20.47	22.42	16.16	14.72	15.90	18.75	19.29	16.75	15.23	13.53	13.62
An	31.80	29.22	28.03	27.12	30.21	30.21	48.48	42.73	32.11	33.64	44.09	42.30	38.47
Di	{wo	14.61	14.96	14.63	14.24	13.32	12.80	10.69	10.84	12.74	12.73	11.53	11.77
	{en	9.59	9.48	9.41	8.63	8.09	7.88	7.02	7.24	8.43	8.51	7.34	8.02
Fs	{wo	3.99	4.52	4.25	4.83	4.50	4.18	2.92	2.79	3.39	3.27	3.43	2.82
	{en	10.97	8.67	8.03	2.73	12.70	12.49	3.59	0.00	7.83	9.74	9.25	11.65
Hy	{fs	4.56	4.13	3.63	1.52	7.07	6.63	1.49	0.00	3.15	4.81	4.32	4.10
	{fs	0.00	1.35	1.73	6.76	0.00	0.00	4.05	6.70	3.92	2.52	0.40	0.10
Fo	0.00	1.35	1.73	6.76	0.00	0.00	4.05	6.70	3.92	2.52	0.40	0.10	0.00
Fa	0.00	0.71	0.86	4.17	0.00	0.00	1.85	2.85	1.73	1.08	0.21	0.03	0.00
Mt	3.40	2.78	3.74	2.55	2.58	3.21	1.75	4.33	3.36	3.95	1.79	2.89	2.95
Ilm	1.93	1.70	2.07	1.86	1.95	1.89	1.12	1.86	1.88	2.18	1.42	1.38	1.84
Ap	0.37	0.25	0.30	0.28	0.25	0.28	0.16	0.44	0.33	0.30	0.25	0.18	0.35

TABLE 5

Mineral and groundmass analyses and partition coefficient of basaltic rocks from the Rift Valley in the Atlantic Ocean near 36°N. (The olivine and plagioclase comprise megacrystic constituents; the pyroxene comprise phenocrysts and matrix constituents)

	Picritic basalts (DR8)		Plagioclase basalts (DR3)			Partition coefficient		
	olivine	glass	plagioc.	pyrox.	matrix	$\frac{\text{olivine}}{\text{glass}}$	$\frac{\text{plagioc.}}{\text{matrix}}$	$\frac{\text{pyrox.}}{\text{matrix}}$
<i>in wt. %</i>								
SiO <sub>2</sub>	40.40	49.50	46.40	49.70	51.0			
Al <sub>2</sub> O <sub>3</sub>	0.15	16.05	33.70	2.15	15.05			
Fe <sub>2</sub> O <sub>3</sub>	11.85	10.80	0.95	7.60	8.80			
MnO	0.75	0.17	0.01	0.14	0.17			
MgO	46.20	9.40	0.20	24.30	7.70			
CaO	0.40	12.95	17.65	16.00	13.35			
Na <sub>2</sub> O	0.00	1.63	1.13	0.29	1.73			
K <sub>2</sub> O	0.08	0.05	0.04	0.00	0.23			
TiO <sub>2</sub>	0.03	0.81	0.04	0.21	1.05			
Total	99.26	100.36	100.12	100.39	99.08			
<i>in ppm</i>								
Ti	180	4,860	240	1,260	6,300	0.037	0.038	0.2
V	20	225	25	185	250	0.088	0.1	0.74
Cr	565	505	5	3,000	230	1.1	0.02	13.0
Mn	1,212	1,324	100	1,083	1,331	0.917	0.07	0.81
Fe	82,950	75,600	6,650	53,000	61,600	1.05	0.1	0.86
Co	121	42	4	53	40	3.0	0.1	1.32
Ni	2,000	165	5	352	80	12.2	0.06	4.4
Cu	11	96	19	20	108	0.11	0.17	0.18
Zn	42	52	8	35	69	0.86	0.11	0.5

for a given temperature [17]. Our data agree with other published analyses (especially Cr and Ni) [18–20] (Table 5). The partition coefficients for olivine, pyroxene and plagioclase are plotted as a function of atomic number (Fig. 3). These plots are qualitatively in agreement with the ligand field theory [21–23]. The highest partition coefficients occur for Cr, Co and Ni in olivine and clinopyroxene, which is in relation to the high stabilization energy in an octahedral environment. Clinopyroxene is more enriched in Ti, V, and Cr (low atomic number) than olivine, and the inverse is observed for high atomic number elements such as Co and Ni (Fig. 3). In all cases, the Ti and V partition coefficients are lower than one, and in a crystallization process the liquid must be enriched in these elements as outlined by Wager and Mitchell [24]. The partition coefficient of Cu (0.1) in pyroxene and olivine agrees with the data of Wager and Mitchell [24]. The partition coefficients

of the plagioclase are near 0.1 (Table 5) for all elements. The bulk rock analyses of the transition metals given in Table 6 are plotted as chondrite normalized values in Fig. 4. The general trend is a “W” shape with Cr and Ni located on the apex of the curves [21]. Variations in concentrations of normalized values are observed for the different basalt types, especially for Ni and Cr which have the highest partition coefficients in olivine and pyroxene. As Cr and Ni decrease, Ti and V increase (partition coefficients <1) but to a smaller extent. Among the transition elements Cr and Ni best differentiate between the different types of basalts encountered.

#### 4.2. Ni–MgO; Cr–Ni; V–Ti variation diagrams

Ni–MgO correlation was shown by Kay et al. [13] and Hedge [25] from geographically dispersed data



RIFT VALLEY IN THE ATLANTIC OCEAN

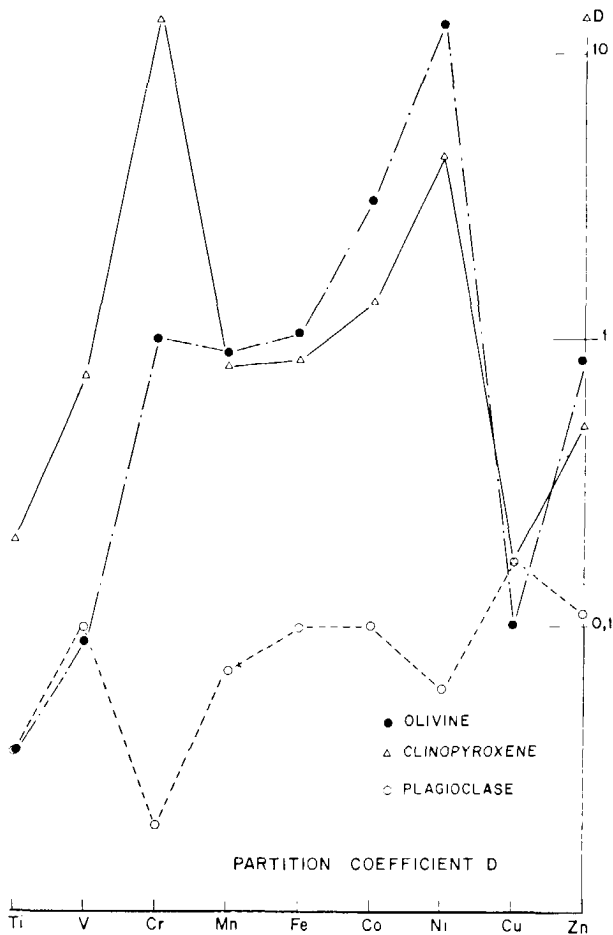


Fig. 3. Partition coefficient diagram of the first transition-series elements versus their atomic number, for olivine, clinopyroxene and plagioclase.

taken from several authors; this diagram presented in Fig. 5 clearly separates the fields of plagioclase, pyroxene and olivine basalts and show the enrichment of Ni in the olivine basalts. Careful consideration must be given to the meaning of a mean value generally chosen as 100 ppm for Ni in basalts because of the possible variation of this element between and within different types.

It is known that for a given magma, as crystallisation proceeds, the concentration of a trace element in the liquid is given by the Rayleigh fractionation law:

$$\frac{C_1}{C_0} = F^{(D-1)}$$

where  $C_1$  = concentration of the element in the liquid,

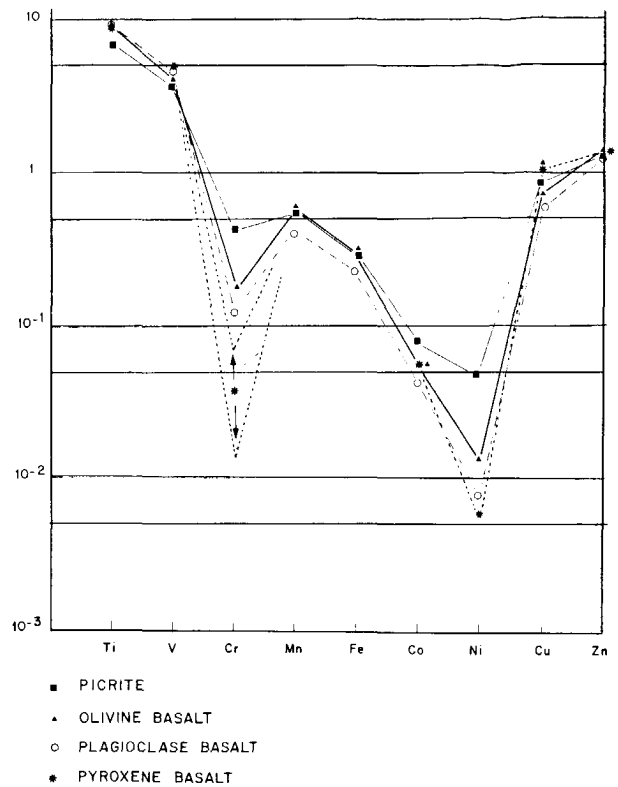


Fig. 4. Chondritic normalized transition metal abundances in the bulk rocks from 36°N.

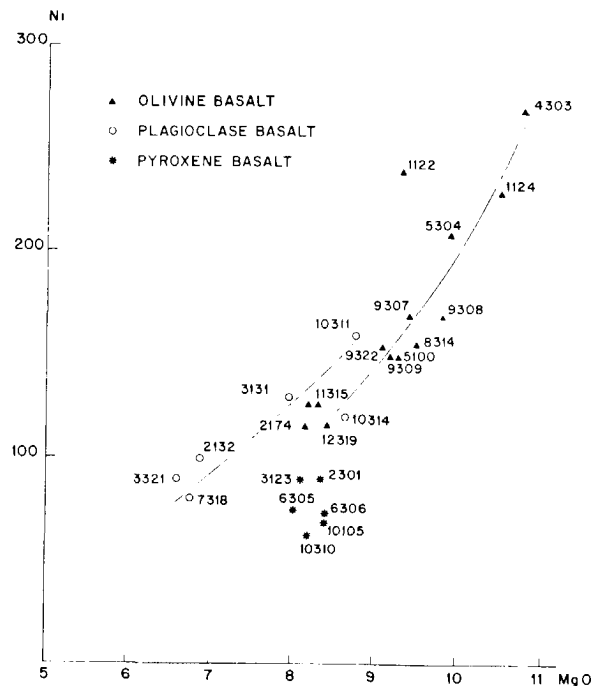


Fig. 5. Ni-MgO diagram of rocks from 36°N. The symbols are the same as in Fig. 2.

TABLE 6  
Transition element analyses (ppm) of bulk rocks from the Rift Valley near 36°N

	Picritic basalts		Olivine basalts												
	DR12	DR12	DR1	DR1	DR4	DR9	DR5	DR9	DR9	DR9	DR8	DR5	DR12	DR11	DR11
	-316	-320	-122	-124	-303	-309	-304	-322 inter.	-322 margin	-308	-314	-100	-319	-315X	-315Y
Ti	3,540	3,100	5,300	5,300	5,100	6,000	6,300	6,100		6,000	6,480	7,550	8,500	8,640	8,570
V	152	200	210	197	182	245	200	250	255	220	238	240	280	243	250
Cr	1,000	1,350	605	550	510	485	460	385	390	380	365	345	260	255	252
Mn	1,240	1,240	1,160	1,240	1,080	1,240	1,160	1,320	1,320	1,320	1,320	1,320	1,400	1,400	1,400
Fe	67,200	68,000	67,100	68,400	64,000	69,500	69,900	74,000	73,400	72,800	74,400	77,100	82,200	83,600	80,700
Co	58	55	33	45	45	45	45	35	33	48	48	48	33	45	42
Ni	650	420	240	230	270	155	210	165	155	170	162	150	125	130	130
Cu	106	95	76	79	89	67	77	67	70	74	72	82	66	67	67
Zn	56	70		66	61	70	69	70	70	68	72	78	70	82	82

TABLE 6 (continued)

	Olivine basalts	Pyroxene basalts					Plagioclase basalts							
	DR2	DR3	DR2	DR6	DR10	DR10	DR6	DR10	DR10	DR10	DR3	DR2	DR7	DR3
	-174	-123	-301	-306	-310	-105	-305	-311	-100	-314	-131	-132	-318	-321
Ti	8,400	5,340	6,030	5,820	5,940	6,120	6,420	5,800	5,750	6,830	4,320	4,500	5,800	3,500
V	250	230	230	255	238	228	255	245	218	222	187	187	245	180
Cr	230	190	145	120	62	62	35	550	430	380	377	280	215	225
Mn	1,400	1,160	1,160	1,320	1,320	1,320	1,240	1,160	1,160	1,240	930	930	1,080	774
Fe	79,000	65,600	66,500	73,700	74,700	73,400	71,300	67,000	62,000	70,400	54,700	51,500	64,300	44,700
Co	45	45	42	45	45	48	45	33	45	42	36	31	33	20
Ni	120	90	90	72	62	72	75	165	120	125	135	100	80	90
Cu	74	98	103	93	79	86	107	67	68	65	72	60	66	47
Zn	80	65	65	70	70	72	70		61	69	51	52		

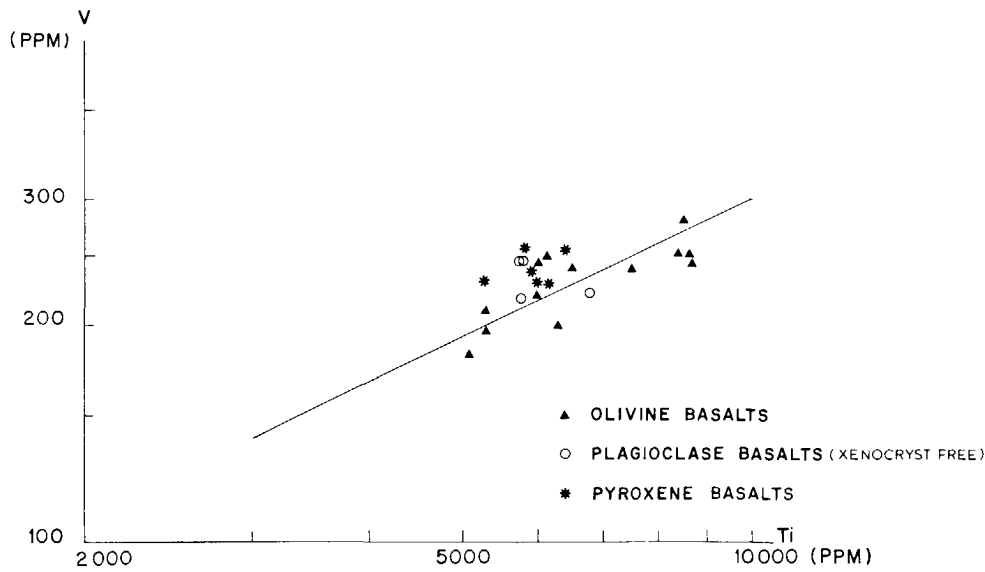


Fig. 6. V-Ti logarithmic correlation diagram of basaltic rocks from 36°N. Only xenocryst-free samples are plotted. The symbols are the same as in Fig. 2.

$C_0$  = initial concentration of the element in the liquid,  $F$  = weight fractionation of liquid that remains,  $D$  = partition coefficient between solid and liquid phase ( $D = C_s/C_l$ ,  $C_s$  being the concentration in the solid).

$$\text{and } \frac{C_s}{C_0} = DF(D-1)$$

Considering two elements, the concentration  $C_s^1$  of the element 1 as a function of the concentration of the element 2 ( $C_s^2$ ) is given by the following relationship:

$$\log C_s^1 = \frac{D^1 - 1}{D^2 - 1} \log C_s^2 + \frac{(D^2 - 1) \log D^1 - (D^1 - 1) \log D^2}{D^2 - 1} + \log \frac{C_0^1}{C_0^2}$$

If  $D^1$  and  $D^2$  representing the bulk partition coefficients remain constant during the crystallisation process, then  $(D^1 - 1)/(D^2 - 1)$  is the slope value of the straight line  $\log C_s^1 = f(\log C_s^2)$ . This implies that the partition coefficients of the minerals and the proportions of minerals crystallizing are constant as crystallization proceeds.

Fig. 6 shows  $\log V$  versus  $\log Ti$  for all samples studied except those containing megacrysts. Vanadium and titanium enter preferentially into pyroxenes and the bulk partition coefficients can be approximated

as to be:

$$D^V = \alpha D_{pyr}^V \text{ and } D^{Ti} = \alpha D_{pyr}^{Ti}$$

$\alpha$  being the proportion of pyroxenes,  $D_{pyr}^V$  and  $D_{pyr}^{Ti}$  being the partition coefficients of these two elements in pyroxene. Giving a value 0.45 to  $\alpha$ , and using the values of the partition coefficient found, the theoretical slope of the curve  $\log V = f(\log Ti)$  is 0.72 which is close to the experimental slope value of 0.65. This concordance would confirm the process of fractional crystallisation only for olivine basalts, since the number of determinations for both the pyroxene basalts and the plagioclase (without megacrysts) are insufficient to draw similar conclusions. Considering the Cr and Ni in the case of the olivine basalts, it is not possible to calculate the theoretical value of the slope as the bulk partition coefficients can be approximated as:

$$D^{Cr} = \alpha D_{pyr}^{Cr} + \beta D_{ol}^{Cr}; \quad D^{Ni} = \alpha D_{pyr}^{Ni} + \beta D_{ol}^{Ni}$$

$D^{Cr}$  and  $D^{Ni}$  cannot be considered as constant because  $\beta$  representing the proportion of olivine in these rocks shows a wide range of variation; hence the Rayleigh law is not valid. This is why  $\log Cr = f(\log Ni)$  is not a straight line (Fig. 7) for olivine basalts. The varia-

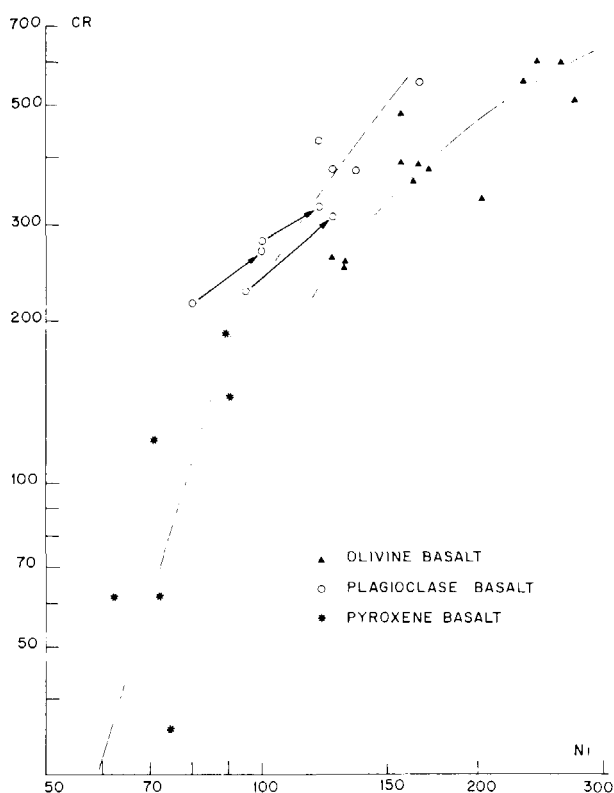


Fig. 7. Cr-Ni logarithmic correlation diagram of basaltic rocks from 36°N. The tie line between two empty circles indicates the recalculated plagioclase basalts megacryst-free values. The symbols are the same as in Fig. 2.

tion of the slope value of the curve  $\log Cr = f(\log Ni)$  is qualitatively in agreement with both the variation of the olivine content and the fractional crystallization process. It is difficult to draw conclusions for plagioclase basalts because of their content of plagioclase megacrysts. Nevertheless the Cr content of the plagioclase basalts is in the same range of variation to that of the olivine basalts. However, the Ni values of the plagioclase basalts are lower than those of the olivine basalts. From the partition coefficient data the distribution of Cr and Ni in these rocks is in agreement with their mineralogical composition.

For pyroxene basalts, the bulk partition coefficients can be approximated as constant (Fig. 7):

$$D^{Cr} \approx \alpha D_{pyr}^{Cr}, D^{Ni} \approx \alpha D_{pyr}^{Ni}$$

The theoretical slope of the curve  $\log Cr = f(\log Ni)$  calculated from partition coefficients and taking a value of  $\alpha = 0.5$  would be 4.5. The experimental value

4.5 + 1 is in good agreement and it can be concluded that the fractional crystallization is responsible for the distribution of these two elements in these rocks. The low Cr content of pyroxene basalts suggests two possible origins for these rocks: (1) the pyroxene basalts crystallized from a separate magma, which may have given rise to chromite precipitation prior to the formation of pyroxene basalts; (2) the pyroxene basalts are considered to be the end product of crystallization of either the plagioclase basalts or the olivine basalts. In this later case the precipitation of chromite is not necessary since pyroxene fractionation from either plagioclase or olivine basaltic types of melt is enough to explain the Cr depletion of the pyroxene basalts.

The Co concentrations remain more or less constant within the different rock types. This is in agreement with the partition coefficients found which lead to a bulk partition of Co near 1 in olivine basalts and 0.7 in plagioclase or pyroxene basalts; in this way the factor  $(D - 1)$  of the Rayleigh law is near 0 and  $C_1$  does not vary significantly.

## 5. Discussion and conclusions

The survey of a limited region of the Rift Valley near 36°50'N revealed the presence of four different types of rocks: picritic basalts with abundant olivine, megacrysts, olivine basalts, highly phyrlic and moderately phyrlic plagioclase basalts and pyroxene basalts.

The distribution of the transition elements observed in the olivine basalts, the pyroxene basalts and the megacryst-free plagioclase basalts is explained by a fractional crystallization process. Because of their heterogeneous composition these three rock types could be the results of crystallization from three different parental magmas. Another possibility is the occurrence of two magma types, one giving rise to olivine basalts, the other to plagioclase basalts. Since it is observed from the Cr concentrations that at the same stage of magmatic evolution either olivine basalts or plagioclase could be produced it is difficult to imagine that both rock types are derived from the same magma. From Cr and Ni data, pyroxene basalts can be seen as end product of crystallization of either plagioclase or olivine basaltic magmas. The Cu content of the pyroxene basalts (~100 ppm) compared to both

## RIFT VALLEY IN THE ATLANTIC OCEAN

the olivine and the plagioclase basalts (~70 ppm) is in agreement with the Cr and Ni data.

The occurrence of different types of basalts is not confined to the 36°N but other provinces of the M.A.R. have similar types of rocks. As far as we know, the basaltic rocks found near 36°N are most similar to those from 45°N [5] in the North Atlantic especially with regard to the enriched potassic rocks (> 0.25%) falling in a narrow TiO<sub>2</sub> range found here in the pyroxene basalts.

### Acknowledgements

This study was possible thanks to the help given by Commandant Priser, the officers and crew on board the R.V. "Jean Charcot" during the 1972 dredging operation in the Rift Valley of the Atlantic Ocean at 36°N. V. Renard (chief scientist) and the other members of the scientific party are gratefully acknowledged. We are particularly indebted to P. Cambon who analysed most of the specimens. Drs. A. Miyashiro and M. Girod have read the manuscript and made valuable comments for its improvement.

### References

- 1 B.C. Heezen, M. Tharp and M. Ewing, The floor of the oceans, I. The North Atlantic, Geol. Soc. Am., Special Paper 65 (1959) 122 pp.
- 2 G. Bellaiche, J.L. Cheminée, J. Francheteau, R. Hekinian, X. Le Pichon, H.D. Needham and B. Ballard, Rift Valley's inner floor: first submersible study, Nature (1974) in press.
- 3 G.D. Nicholls, Basalts from the deep-ocean floor. Mineral Mag. 34 (1965) 373-388.
- 4 I.D. Muir and C.E. Tilley, Basalts from the northern part of the Mid-Atlantic Ridge, II. The Atlantis collections near 30°N, J. Petrol. 7 (1966) 193-201.
- 5 F. Aumento, The Mid-Atlantic Ridge near 45°N, II, Basalts from the area of Confederation Peak, Can. J. Earth Sci. 5 (1967) 1-21.
- 6 H.D. Needham and J. Francheteau, Some characteristics of the Rift Valley in the Atlantic ocean near 36°48' North, Earth Planet. Sci. Lett. 22 (1974) 29-43.
- 7 R. Hekinian, M. Chaigneau and J.L. Cheminée, Popping rocks and lava tubes from the Mid-Atlantic Rift Valley at 36°N, Nature 245 (1973) 371-373.
- 8 F. Shido, A. Miyashiro and M. Ewing, Crystallization of abyssal tholeiites, Contrib. Mineral. Petrol. 31 (1971) 251-226.
- 9 R. Hekinian and F. Aumento, Rocks from the Gibbs fracture zone and the Minia Seamount near 53°N in the Atlantic Ocean, Mar. Geol. 14 (1973) 47-72.
- 10 A. Miyashiro, F. Shido and M. Ewing, Diversity and origin of abyssal tholeiites from the Mid Atlantic Ridge near 24 and 30°N latitude, Contrib. Mineral. Petrol. 23 (1969) 38-52.
- 11 E.F. Osborn and D.B. Tait, The system diopside-forsterite-anorthite, Am. J. Sci., Bowen, (1952) 413-433.
- 12 W.C. Melson and G. Thompson, Petrology of a transform fault zone and adjacent ridge segments, Phil. Trans. R. Soc. Lond. A 268 (1971) 423-441.
- 13 R.Kay, H.J. Hubbard and P. Gast, Chemical characteristics and origin of oceanic ridge volcanic rocks, J. Geophys. Res. 75 (1970) 1585-1613.
- 14 W.G. Melson and G. Thompson, Glassy abyssal basalts, Atlantic sea floor near St-Paul's rocks: petrography and composition of secondary clay minerals, Geol. Soc. Am. Bull. 84 (1973) 703-716.
- 15 A. Poldervaart and J. Green, Chemical analyses of submarine basalts, Am. Mineral. 50 (1965) 1723-1727.
- 16 F. Albarède and Y. Bottinga, Kinetic disequilibrium in trace element partitioning between phenocrysts and host lava, Geochim. Cosmochim. Acta 36 (1972) 141-156.
- 17 T.A. Hakli and J.L. Wright, The fractionation of nickel between olivine and augite as a geothermometer, Geochim. Cosmochim. Acta 31 (1967) 877-884.
- 18 P.W. Gast, Trace element fractionation and the origin of tholeiitic and alkaline magma types, Geochim. Cosmochim. Acta 32 (1968) 1057-1086.
- 19 T.A. Hakli, An attempt to apply the Makaopuhi nickel fractionation data to temperature determination of a basic intrusive, Geochim. Cosmochim. Acta 32 (1968) 449-460.
- 20 S.M. Dale and P. Henderson, The partition of transition elements in phenocryst bearing basalts and the implications about melt structure, 24th IGC (1972) Section 10.
- 21 C.J. Allègre, M. Javoy and G. Michard, Etude de la distribution et de l'abondances des éléments de transition dans l'écorce terrestre comparées à celles des terres rares, in: Origin and Distribution of the Elements, ed. L.H. Ahrens (Pergamon Press, 1968) 913-928.
- 22 G. Burns, Mineralogical applications of crystal field theory (Cambridge Earth Sci. Series, Cambridge Univ. Press, 1970) 224 pp.
- 23 L.E. Orgel, Chimie des éléments de transition (Dunod, Paris, 1964).
- 24 L.R. Wager and R.L. Mitchell, The distribution of trace elements during strong fractionation of basic magma; a further study of the Skaergaard intrusion, East Greenland, Geochim. Cosmochim. Acta 1 (1951) 129-208.
- 25 C.E. Hedge, Nickel in high-alumina basalts, Geochim. Cosmochim. Acta 35 (1971) 522-524.